

0.1 ml of 20 percent formaldehyde. The platelets were harvested by centrifugation at 12,000g for 25 minutes. After decanting the supernatant, the platelets were digested in hydrogen peroxide and poured into scintillation vials for liquid scintillation spectrometry. The amount of serotonin that accumulated at 4°C was subtracted from each sample.

7. J. J. Schildkraut, S. M. Schanberg, G. R. Breese, I. J. Kopin, *Am. J. Psychiatry* **124**, 600 (1967).
8. M. Asberg, L. Bertilsson, D. Tuck, B. Cronholm, F. Sjoqvist, *Clin. Pharmacol. Ther.* **14**, 277 (1973).

22 July 1977

Silicon Identification in Prosthesis-Associated Fibrous Capsules

Abstract. *The use of correlated microscopic techniques, including the scanning electron microscopic modes of backscattered electron imaging and energy dispersive x-ray analysis, aid in defining the process of dispersion of silicon-containing material around silicone rubber (polydimethylsiloxane) prosthetic devices.*

Fibrous capsule formation after the implantation of a relatively large, inert object in tissue is a basic wound-healing response. Breast prosthesis implantation in humans, a major surgical market for silicone prostheses, generates a capsule which, when contracted (1-3), affects the success of mammary augmentation. Contraction of the breast capsule causes disfigurement or pain, or both, often leading to further surgery or even to the removal of the prosthesis and implantation of a new device. Although silicone breast prostheses have had extensive clinical use for more than 10 years, the conditions leading to a poor clinical course have not been systematically or experimentally evaluated by using adequate scientific techniques.

The polydimethylsiloxane polymers (silicone rubber) used in the construction of all types of currently used prosthetic devices may undergo substantial change

once they are localized at a tissue site (4-6). Electron microscopic studies (2, 7) have described unique intra- and extracellular vacuoles associated with breast implants. To date, the in situ localization of silicon in those vacuoles has not been proved. The only precise identification of silicon in previous studies has been with standard bulk chemical spectroscopic techniques. The literature contains a single case report (8) of the identification of polydimethylsiloxane by atomic absorption spectrophotometry in human tissues. Infrared and ultraviolet spectroscopy have been used in experimental studies (3).

The data presented here are, to our knowledge, the first that conclusively demonstrate both cell-localized and extracellular silicon-containing material away from a polydimethylsiloxane implant. We were able to obtain these data only by using optical visualization and

spectrometry in combination. Our study indicates that while the techniques of transmission electron microscopy are useful for describing the relationship between prosthesis-associated materials and the cells or tissues within which they are contained, the scanning electron microscopy (SEM) procedures of backscattered electron imaging and energy dispersive x-ray analysis (EDXA) identify and demonstrate the exact extent of silicon-containing material within tissue blocks. The SEM procedures have been used in other diagnostic applications, including the identification of inorganic silicon compounds (9), and their use by investigators working with any formulation of polydimethylsiloxane should provide a more accurate analysis of the movement of silicon-containing material away from a silicon-based device. More importantly, possible differences in electron scatter or differential x-ray intensities might allow the discrimination and identification of the source of tissue-localized material.

Ten fibrous capsule biopsies were obtained at the time of reimplantation of gel-filled mammary augmentation devices. The devices consisted of a silicone rubber envelope surrounding a less viscous silicone gel. All of the long-term prosthetic devices removed were intact and were grossly similar to the new implants. In one case the prosthesis removed at the time of resurgery was also taken. All samples, including a section of the prosthesis, were first fixed in an alde-

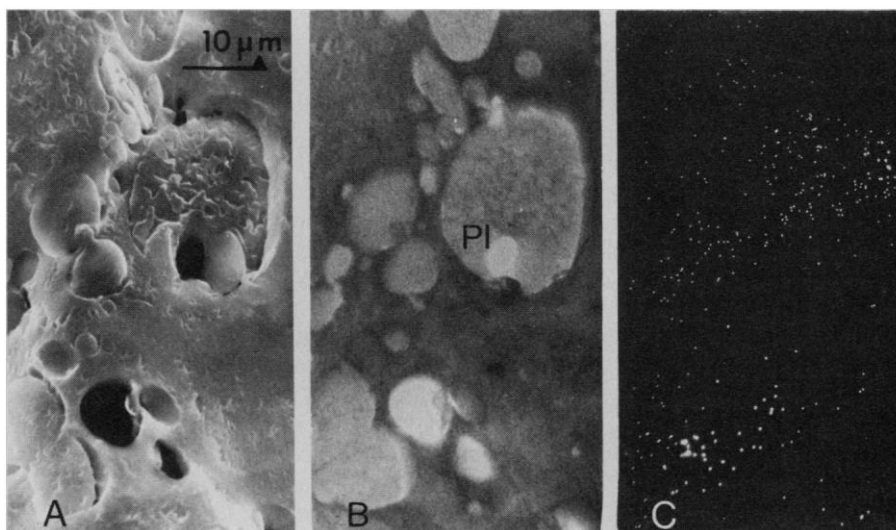
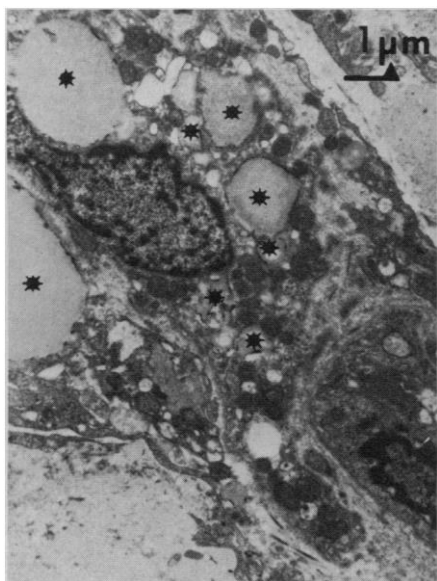


Fig. 1 (left). Transmission electron micrograph illustrating a diverse assortment of vacuoles (*) presumed to contain silicone and apparently located within a contracted capsule fibroblast (x

6500). Fig. 2 (right). Series of scanning electron micrographs of a thick section adjacent to the thin section shown in Fig. 1: secondary electron (A), backscattered electron (B), and EDXA (C) modes. The backscattered electron image here, and the one in Fig. 4B, are shown with reversed signal polarity to facilitate comparison with the more familiar transmission electron microscopic image. Regions of higher atomic number thus appear darker because of greater electron scatter. The EDXA silicon map demonstrates the presence of silicon localized in the vacuoles. Other elements (Cl, Os, U, and As) present in the sections were not selectively distributed. Point PI is the site of the spectral peak intensity analysis (x 1100).

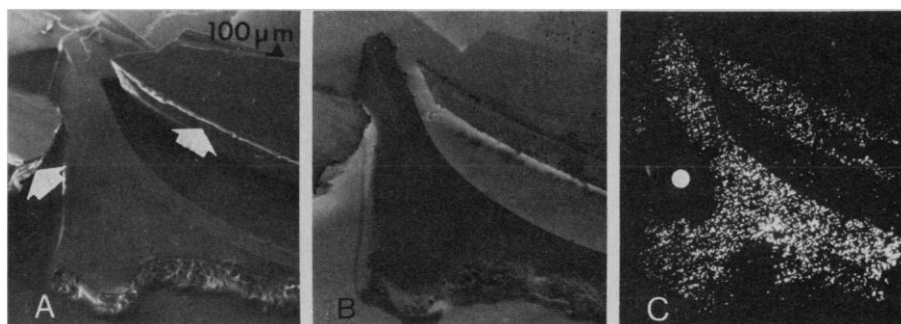
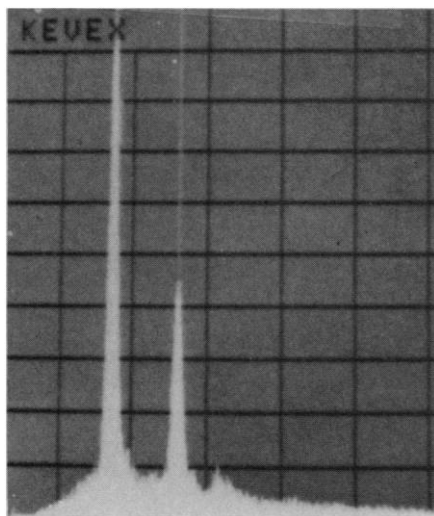


Fig. 3 (left). A spectrum of peak intensity (EDXA) showing silicon (1.74 keV) at point *PI* in Fig. 2B. The presence of chlorine (2.63 keV) indicates that the material in the vacuole was embedded in chlorine-rich epoxy resin. This 20-second analysis was done at 20 kv with a specimen current of 0.5 na. The ordinate shows the number (0 to 1000 counts) and the abscissa the energy (0 to 5 keV) of the x-rays detected.

Fig. 4 (right). Series of scanning electron micrographs illustrating the different imaging characteristics of a section of silicone breast prosthesis with secondary electron (A) and backscattered electron (B) imaging and the silicon distribution in the same section with EDXA (C). The arrows in (A) indicate the faces of the confining Epon block that have fallen away from the prosthesis. The dot in (C) indicates an artifactual area lacking the silicon signal, caused by the absorption of x-rays at an Epon fragment lying between the sample and the x-ray detector ($\times 19$).

hyde (4 percent paraformaldehyde and 5 percent glutaraldehyde) fixative in 0.1M cacodylate buffer at pH 7.45. The samples were then postfixed in 2 percent osmium tetroxide in the same buffer, stained en bloc with 2 percent uranyl acetate, dehydrated, and embedded in an Epon 812 resin mixture.

Stained sections were examined by light (toluidine blue) and transmission electron (lead citrate) microscopy. The resulting photomicrographs were examined in a single-blind fashion by one of us (M.G.W.) and the samples were divided into three categories based on the abundance of vacuoles. Tissues in the first group (six of the ten samples) demonstrated the distinctive vacuoles associated with presumed polydimethylsiloxane localization (2, 7). Those in the second category (two of ten) had traces of that material, and those in the third (two of ten) showed no such material. A piece of the periphery of the prosthesis constituted a fourth category. Sections 4 μ m thick were taken from the representative blocks, glued to carbon planchets, and examined in a double-blind manner by one of us (J.L.A.) with an ETEC scanning electron microscope using secondary electron, backscattered electron (10), and energy dispersive x-ray analysis modes.

The light and transmission electron (Fig. 1) microscopy results for biopsies with vacuoles show intra- and extracellular droplets composed of an amorphous material similar to that previously described (2). Not all of the deposits were visible at the light microscopic level. The SEM observations on correlated sections provide certain identification of vacuoles seen in transmission electron micrographs. Both second-

ary electron imaging (Fig. 2A) and backscattered electron imaging (Fig. 2B) demonstrate droplets with the latter providing a more distinctive outline of droplet features and distribution. EDXA results show the localized presence of silicon in suspect vacuoles either by distribution mapping (Fig. 2C) or by spectral peak intensity analysis (Fig. 3).

The differential distribution of silicon (that is, that it was limited to the droplets) was repeatedly demonstrated. The SEM observations also showed a lack of silicon-containing material in tissue previously found to be lacking in the characteristic vacuoles.

The silicon-containing material demonstrated in biopsy material seemed more uniform than that in the prosthesis. The prosthesis, like the material contained in the tissue, was osmiophilic and we were able to contain a piece of it within an Epon block by enveloping it in the plastic. Even then we were able to get thick sections of it only with difficulty. In the scanning electron microscope we were able to visualize a denser 100- μ m-thick layer underlaid by a less dense layer (Fig. 4, A and B). Silicon was identified in the prosthesis sample and on the confining faces of Epon block (Fig. 4C) in EDXA results. The outer layer of the device differed from the inner material in electron scatter, reflecting the presence of a nominal 20 percent silica (SiO_2) filler in the envelope only (11).

Organic silicon compounds, unlike inorganic ones, have not been objectively linked in a cause-effect relationship with observed pathology. Since polydimethylsiloxane structural devices are invaluable in reconstructive and therapeutic surgery, immediate attention should

be given to verifying the apparently benign nature of this material by using appropriate analytical techniques. However, such analyses must be done with caution because, in addition to its use in many different types of structural prosthetic devices, polydimethylsiloxane serves a major function as a lubricant in disposable syringes. Only by taking care in handling samples to avoid postmortem or postbiopsy contamination with environmental silicon compounds and by using correlated microscopy techniques centered around EDXA will it be possible to obtain objective information on the distribution and effects of polydimethylsiloxane in the body.

M. GARY WICKHAM

ROSS RUDOLPH

Research Service, Veterans Administration Hospital, and Department of Surgery, University of California, San Diego 92161

JERROLD L. ABRAHAM

Department of Pathology, University of California, San Diego 92093

References and Notes

1. J. E. Williams, *Plast. Reconstr. Surg.* **49**, 253 (1972).
2. P. Wilflingseder, A. Propst, G. Mikuz, *Chir. Plast.* **2**, 215 (1974).
3. R. Gayou, *McGhan Medical Report No. 2201* (McGhan Medical Corp., Santa Barbara, Calif., 1976).
4. E. Roggendorf, *J. Biomed. Mater. Res.* **10**, 123 (1976).
5. E. F. Cuddihy, J. Moacanin, E. J. Roschke, E. C. Harrison, *ibid.*, p. 471.
6. R. H. Rigdon and A. Dricks, *ibid.* **9**, 645 (1975).
7. E. J. Domanskis and J. Q. Owsley, Jr., *Plast. Reconstr. Surg.* **58**, 689 (1976).
8. E. T. Solomons and J. K. Jones, *J. Forensic Sci.* **20**, 19 (1975).
9. J. L. Abraham, in *IITRI Scanning Electron Microscopy/1977* (IIT Research Institute, Chicago, 1977), vol. 2, p. 119.
10. _____ and P. B. DeNee, in *IITRI Scanning Electron Microscopy/1974* (IIT Research Institute, Chicago, 1974), p. 251.
11. Finely ground particles (10 nm in diameter) of

amorphous SiO₂ are added to the envelope of the device to enhance its structural strength; they comprise 20 to 30 percent of the envelope. Before we received this information (from E. Frisch, Dow Corning Company, Midland, Mich.), we had noted that the envelope gave consistently higher Si counts per second (cps) than did the contained gel. Typical Si counting rates were 1480 ± 20 cps in the gel and 1520 ± 30 cps in the envelope. We did not feel that this apparent difference in silicon volume was due to pack-

ing density alone and hypothesized the presence of another silicon-containing compound to explain the difference in the Si contribution to formula weight (37.9 percent at 1480 cps compared to 39.11 percent at 1520 cps).

12. We appreciate the capable assistance of M. Woodward and S. Guber. Supported by the San Diego Veterans Administration Hospital Research Service and PHS grant HL 19619.

20 September 1977; revised 8 November 1977

Cretaceous Bivalve Larvae

Abstract. *Exceptionally well preserved larval bivalve shells have been isolated from Late Cretaceous (Maestrichtian) sediments. Specimens were readily identified to familial level on the basis of gross morphology and hinge structures. Reconstruction of fossil larval ontogeny, linked with the distribution of adult stages, will provide an important interpretative tool in molluscan phylogenetic and paleoecologic studies.*

Identification of bivalve larvae has been the subject of biological research for over a century (1). Despite the paleontological implications of diagnostic larval shell characters, studies to date have dealt almost exclusively with extant species. Larval shells are small and fragile, and, in ancient sediments, have generally been assumed to have been destroyed mechanically or by chemical dissolution. In a pathfinding study, LaBarbera (2) described the larval and post-larval development of five species of "Miocene" bivalves (3), but his specimens were obtained from sediment retained on a 500- μ m diagonal mesh screen. Accordingly, his descriptions of larval ontogeny were based predominantly on prodissoconch characteristics observed on the surface of ontogenetically metamorphosed juveniles; postmetamorphic growth obscured primary larval dentition in the majority of specimens examined. In the present study, disarticulated Cretaceous larval bivalve shells have been isolated from the 125- to 500- μ m sediment fraction and identified to familial level on the basis of gross morphology and hinge structures.

In searching for juvenile fossil mollusks, collections were made at a number of Late Cretaceous localities exhibiting unusually good preservation of fossil material (4). Bulk samples from the Monmouth Formation (Maestrichtian) near Brightseat, Maryland (5), were wet-sieved through a standard Udden-Wentworth sieve series, and the 125- and 250- μ m fractions were examined with a dissecting microscope ($\times 50$). Larval and early postmetamorphic bivalve shells were removed from the sample with a fine brush (6) and carefully mounted on copper conducting tape. Specimens were subsequently coated with gold-palladium (approximately 200 Å thick) in a Polaron diode sputtering system and examined

with a scanning electron microscope (ETEC Autoscan).

Cretaceous larval shells, once isolated, have proved to be more than adequately well preserved for identification. The bivalve larval characteristics most useful in routine plankton identifications have been shell length, height, and

depth, as well as length of the prodissoconch I hinge line (1, 7-9). Rees (10) discusses at length the usefulness of larval hinge structures in identification studies for superfamilial separation. More recently, workers have used both optical and scanning electron microscopy to describe in detail the hinge structures of several bivalves and have suggested that such structures may be diagnostic at the generic or even specific level (11, 12). These diagnostic larval shell characters have been found to be extremely well preserved in fossil specimens. For example, the Cretaceous larval shell in Fig. 1, A to C, may be placed in the family Pholadidae on the basis of (i) characteristic pholadacean larval hinge apparatus (10, 12); (ii) height approximately equal to length; (iii) relatively prominent "knobby" umbo [in the sense of Chanley and Andrews (7)]; and (iv) broad, flattened internal shell margin (7, 12). Other specimens, such as larval mytilids (Fig. 1D), may be unambiguously identified at the familial level on the basis of hinge structure alone (10, 13). Well-pre-

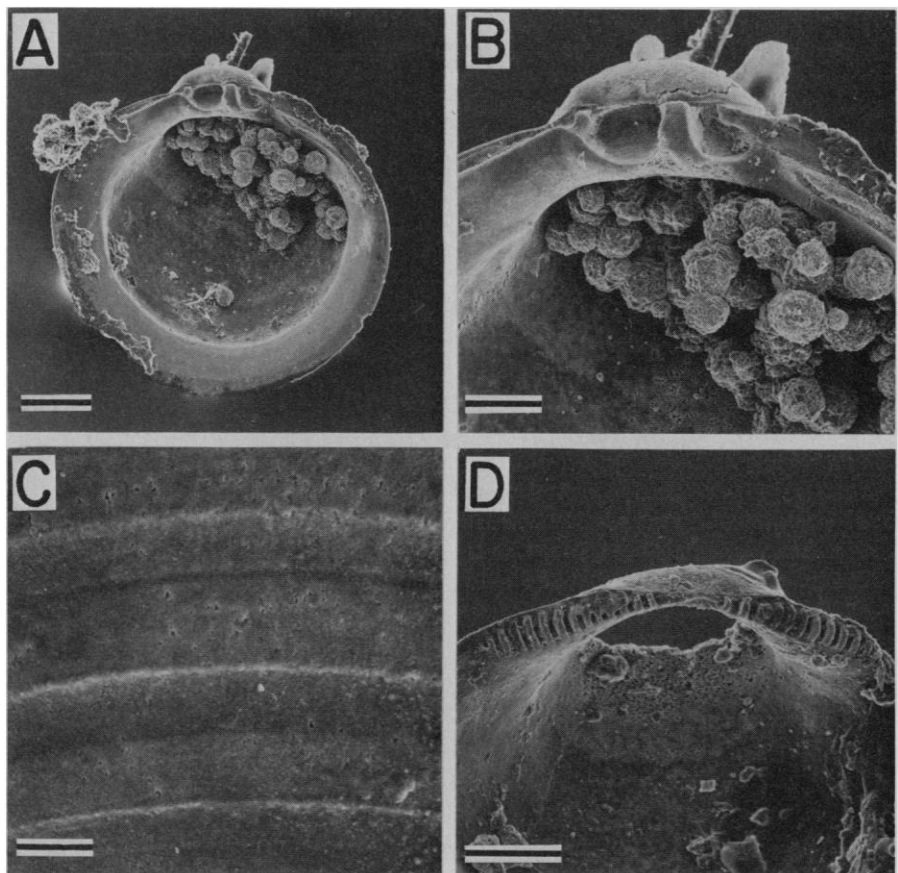


Fig. 1. Scanning electron micrographs. (A) Disarticulated shell valve of a Cretaceous bivalve larva from the Monmouth Formation near Brightseat, Maryland. Larval dentition, length by height (195 by 195 μ m) relation, and umbo shape are characteristic of the family Pholadidae. Framboidal pyrite is seen partially filling shell interior (scale, 40 μ m). (B) Enlargement of hinge apparatus of larval valve seen in (A) showing characteristic pholadacean dentition (scale, 20 μ m). (C) External shell surface of larval pholad seen in (A). Note fine concentric sculpture (scale, 5 μ m). (D) Hinge apparatus (provinculum) of a Cretaceous larval mytilid (shell length, 190 μ m) from the Monmouth Formation (scale, 30 μ m).